

# Modelling of the pulsed field magnetization of HTS bulks in solid nitrogen at 40 K

Ghazi Hajiri

Université de Lorraine, GREEN  
F-54000 Nancy, France  
[0000-0003-0325-0788](mailto:0000-0003-0325-0788)

Kévin Berger

Université de Lorraine, GREEN  
F-54000 Nancy, France  
[0000-0001-8841-917X](mailto:0000-0001-8841-917X)

Jean Lévêque

Université de Lorraine, GREEN  
F-54000 Nancy, France  
[0000-0002-1975-4860](mailto:0000-0002-1975-4860)

**Abstract**—To date, the pulsed field magnetization (PFM) method is considered one of the most promising magnetization methods due to its low cost and flexibility to magnetize samples within the final system. In addition, REBCO bulks with an operating temperature below 77 K are increasingly used in electrical machine applications, where cooling is primarily provided by a closed helium cold loop. In the same context, solid nitrogen (SN<sub>2</sub>) can provide a stable cryogenic environment for magnetizing several bulks simultaneously. This paper discusses the magnetothermal study and modelling of the magnetization of several REBCO bulk samples during their magnetization. For the electromagnetic calculation, the A-H formulation is used, coupled with a thermal model where the solid-liquid phase change of nitrogen has been considered. 2D and 3D numerical results will be compared in the final paper. Furthermore, the results will be compared and validated with experimental measurements.

**Keywords**—HTS bulks, A-H formulation, phase change modelling, cryogenics.

## I. INTRODUCTION

Since the manufacturing and commercialization of superconducting bulks, several methods have been used for their magnetization, among which the so-called field cooling and zero field cooling methods. Alternatively, the pulsed field magnetization (PFM) method is considered the most common method to magnetize bulks inside a superconducting machine, due to its low cost and flexibility [1]–[3].

Within this context, several investigations have been conducted at liquid nitrogen temperature and atmospheric pressure, where the magnitude of the magnetic field trapped in the bulk was limited by the critical current density of the sample at 77 K [4]. At very low temperatures, other research employs direct conduction cooling where the cooling of the system relies on the use of one or more cryocoolers for the high temperature superconducting (HTS) bulks and the magnetizing coil [5]. In this regard, solid nitrogen (SN<sub>2</sub>) can create both a homogeneous thermal environment for cooling and great flexibility for testing multiple and various samples. In addition, solid nitrogen can be used as a thermal buffer to improve the thermal stability of superconducting systems under transient heating circumstances [6].

Recently, the stability of the 3D A-H formulation has been validated and discussed several times [7]–[9]. So far, the coupling of the A-H formulation with thermal equations is typically based on the use of a convection coefficient  $h$  in case the superconducting material is immersed in a liquid, or by means of a thermal resistance if a cryocooler is used. In this work where the superconducting samples are embedded in solid nitrogen, the thermal equations are based on a solid-to-liquid phase change formulation and coupled with the A-H formulation. Moreover, the results of the final 3D coupled A-H formulation will be compared with experimental

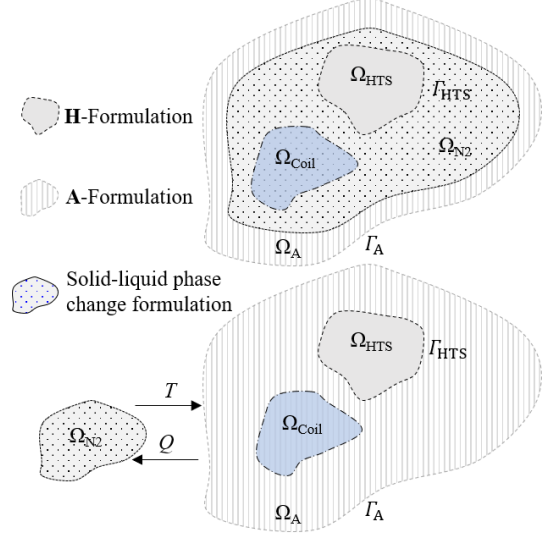


Fig 1. Breakdown of the studied domains and thermal coupling: the bulk  $\Omega_{HTS}$ , the coil  $\Omega_{Coil}$ , the nitrogen  $\Omega_{N2}$  and the air  $\Omega_A$ . The boundaries between the superconductor and the air are denoted  $\Gamma_{HTS}$  and the boundary of the air formulation is  $\Gamma_A$ .

measurements. The cooling system and process are thoroughly described in [10].

## II. MODELLING

The set of equations was implemented and solved using COMSOL Multiphysics 5.6.

### A. A-H formulation

The coupled A-H formulation is based on the resolution of a magnetic vector potential  $\mathbf{A}$  equation in domains such as air and conductors and a magnetic field  $\mathbf{H}$  equation in superconducting parts only. As shown in Fig. 1, the H-formulation (Hf) is used in the  $\Omega_{HTS}$  superconducting domain, where the equation to be solved can be written as follows:

$$\mu_0 d_t \mathbf{H}_{Hf} + \nabla \times (\rho \nabla \times \mathbf{H}_{Hf}) = 0 \quad \mathbf{H}_{Hf} \in \Omega_{HTS} \quad (1)$$

The A-formulation (Af) is applied in the coil  $\Omega_{Coil}$  and air  $\Omega_A$  domains, where the vector potential  $\mathbf{A}$  is defined by  $\mathbf{B}_{Af} = \nabla \times \mathbf{A}_{Af}$ . The equations to be solved can be written as:

$$\nabla \times (\mu_0^{-1} \nabla \times \mathbf{A}_{Af}) = \mathbf{J}_{Coil} \quad \mathbf{A}_{Af} \in \Omega_{Coil} \quad (2)$$

$$\nabla \times (\mu_0^{-1} \nabla \times \mathbf{A}_{Af}) = 0 \quad \mathbf{A}_{Af} \in \Omega_A \quad (3)$$

The coupling between the two formulations Af and Hf is provided by a vector equality of the magnetic field at the boundary between the two domains, i.e.,  $\Gamma_{HTS}$  in the case studied. In order to ensure the continuity of the physical quantities, the Neumann conditions are used, and the coupling equations can be expressed in the form:

$$\mathbf{n} \times \mathbf{H}_{Hf} = \mathbf{n} \times (\mu_0^{-1} \nabla \times \mathbf{A}_{Af}) \quad \text{on } \Gamma_{HTS} \quad (4)$$

$$\mathbf{n} \times (-d_t \mathbf{A}_{Af}) = \mathbf{n} \times (\rho \nabla \times \mathbf{H}_{Hf}) \quad \text{on } \Gamma_{HTS} \quad (5)$$

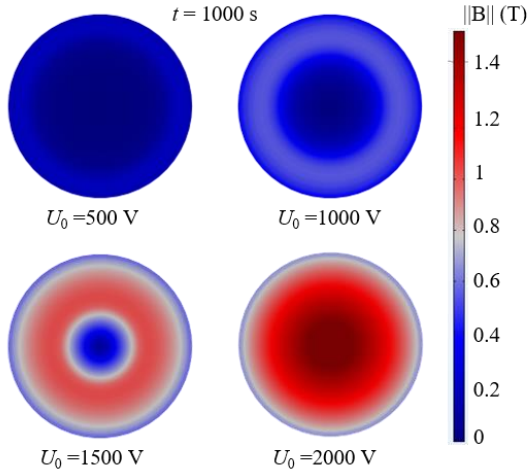


Fig. 2. Distribution of the magnetic flux density norm at the top surface of a REBCO bulk placed in SN<sub>2</sub> at 40 K at the end of the PFM process and for different values of the capacitors charging voltage  $U_0$ .

### B. Thermal equation

To account for thermal effects during magnetization, the heat diffusion equation is implemented in each domain as follows:

$$\gamma C_p \frac{dT}{dt} + \nabla \cdot (-k \nabla T) = \begin{cases} Q_{\text{HTS}} & T \in \Omega_{\text{HTS}} \\ Q_{\text{Coil}} & T \in \Omega_{\text{Coil}} \\ 0 & T \in \Omega_{\text{N}_2} \end{cases} \quad (6)$$

with  $k$  the thermal conductivity,  $C_p$  the specific heat and  $\gamma$  the material density. Furthermore, in each domain  $\Omega_{\text{HTS}}$  and  $\Omega_{\text{Coil}}$ , we define the losses per unit of volume  $Q_{\text{HTS}}$  and  $Q_{\text{Coil}}$  respectively.

### C. Solid-liquid phase change

The heat capacity formulation is implemented to consider the solid-liquid phase change. The principle consists of adding the latent heat  $L$  to the heat capacity when the material reaches its phase change temperature  $T_{\text{SN}_2 \rightarrow \text{LN}_2}$ . Moreover, the transformation from the solid to the liquid state takes place in a temperature interval  $\Delta T$  around  $T_{\text{SN}_2 \rightarrow \text{LN}_2}$ . In order to account for the material property in its proper state, two smooth functions  $\theta_{\text{SN}_2}$  and  $\theta_{\text{LN}_2}$  are defined. As an example,  $\theta_{\text{SN}_2}$  is equal to 1 before  $T_{\text{SN}_2 \rightarrow \text{LN}_2} - \Delta T/2$  and 0 after  $T_{\text{SN}_2 \rightarrow \text{LN}_2} + \Delta T/2$ , and inversely true for  $\theta_{\text{LN}_2}$ . In other words, the sum  $\theta_{\text{SN}_2} + \theta_{\text{LN}_2}$  is always equal to 1.

$$k = \theta_{\text{SN}_2} k_{\text{SN}_2} + \theta_{\text{LN}_2} k_{\text{LN}_2} \quad (7)$$

$$C_p = \left( \frac{1}{\gamma} (\theta_{\text{SN}_2} \gamma_{\text{SN}_2} C_{p\text{SN}_2} + \theta_{\text{LN}_2} \gamma_{\text{LN}_2} C_{p\text{LN}_2}) \right) \quad (8)$$

$$\gamma = \theta_{\text{SN}_2} \gamma_{\text{SN}_2} + \theta_{\text{LN}_2} \gamma_{\text{LN}_2} \quad (9)$$

In a constant pressure phase change,  $\beta_{\text{N}_2}$  represents the mass ratios between the liquid and the solid states, it can be represented as a function of the different density and smooth function  $\theta_{\text{SN}_2}$  and  $\theta_{\text{LN}_2}$ .

$$\beta_{\text{N}_2} = \frac{1}{2} \frac{\theta_{\text{LN}_2} \gamma_{\text{LN}_2} - \theta_{\text{SN}_2} \gamma_{\text{SN}_2}}{\theta_{\text{LN}_2} \gamma_{\text{LN}_2} + \theta_{\text{SN}_2} \gamma_{\text{SN}_2}} \quad (10)$$

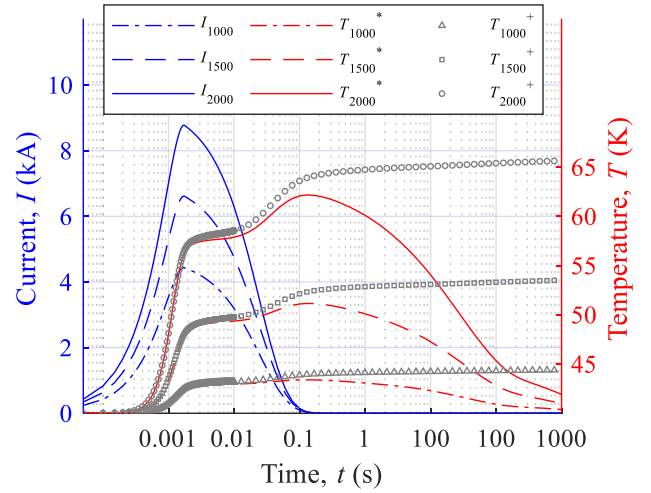


Fig. 3. Current pulse and average temperature of the bulk versus time for different values of  $U_0$  equal to 1000 V, 1500 V and 2000 V. Two average temperatures of the bulk are shown:  $T^*$  is given according to the phase change formulation and  $T^+$  is under adiabatic conditions.

## III. RESULTS AND CONCLUSION

In this section, the magnetization of a REBCO bulk is modelled within an axisymmetric 2D problem. The bulk has a radius of 15.2 mm and a height of 17 mm. The power law  $E(J)$  as well as the dependence of the critical current on the magnetic field and the temperature  $J_c(\mathbf{B}, T)$  have been considered. The current pulse is provided by the discharge of a 5 mF capacitor and an initial charge voltage  $U_0$  that can reach up to 2000 V. To consider the electrical components of the magnetization system [11], the electrical equations of the magnetizer were integrated within the  $\mathbf{A-H}$  formulation. Fig. 2 shows the influence of the discharge voltage on the distribution of the trapped magnetic flux density at the top surface of the REBCO bulk placed in solid nitrogen at 40 K at the end of the PFM process, i.e.  $t = 1000$  s.

Fig. 3 shows the current pulse and the average temperature of the bulk during a PFM for different values of the capacitors charging voltage  $U_0$  of 1000 V, 1500 V and 2000 V. In addition, the average temperature of the bulk calculated by using the solid-liquid phase change formulation and under adiabatic conditions are shown. One can note that during the current rise before  $t = 2$  ms, the temperatures of both models are similar, this is related to the fact that the thermal time constants are considerably higher than the electrical ones. This behavior can offer advantages for 3D simulations. Indeed, to decrease the computation time, during the current rise, the solving of the thermal equations can be considered only in  $\Omega_{\text{Coil}}$  and  $\Omega_{\text{HTS}}$  under adiabatic conditions. The phase change formulation in  $\Omega_{\text{N}_2}$  can then be applied after 2 ms with the appropriate initial conditions observed at the end of the adiabatic regime.

In the final version of the paper, the behavior of solid nitrogen during the application of multiple pulses will be examined. In addition, a coupled 3D model concerning the magnetisation of a set of several bulks will be detailed and compared to the experiment.

## REFERENCES

- [1] Z. Huang, M. Zhang, W. Wang, and T. A. Coombs, "Trial Test of a Bulk-Type Fully HTS Synchronous Motor," *IEEE Transactions on Applied Superconductivity*, vol. 24, no. 3, pp. 1–5, Jun. 2014, doi: 10.1109/TASC.2013.2296142.

- [2] J. Arnaud, J. F. P. Fernandes, and P. J. C. Branco, "Modifying the Pulsed-Field-Magnetization Technique for HTS Bulks in Electrical Machines Without Magnetic Field Sensors," *IEEE Transactions on Applied Superconductivity*, vol. 28, no. 4, pp. 1–4, Jun. 2018, doi: 10.1109/TASC.2018.2801323.
- [3] Z. Deng *et al.*, "Pulsed Field Magnetization Properties of Bulk RE-Ba-Cu-O as Pole-Field Magnets for HTS Rotating Machines," *IEEE Transactions on Applied Superconductivity*, vol. 21, no. 3, pp. 1180–1184, Jun. 2011, doi: 10.1109/TASC.2010.2085071.
- [4] T. Ida, Z. Li, M. Miki, M. Watasaki, and M. Izumi, "Waveform Control Pulse Magnetization for HTS Bulk With Flux Jump," *IEEE Transactions on Applied Superconductivity*, vol. 28, no. 4, pp. 1–5, Jun. 2018, doi: 10.1109/TASC.2018.2816099.
- [5] K. Yokoyama and T. Oka, "Influence of the Shape of Soft-Iron Yoke on Trapped Field Performance of HTS Bulk," *IEEE Transactions on Applied Superconductivity*, vol. 30, no. 4, pp. 1–5, Jun. 2020, doi: 10.1109/TASC.2020.2976064.
- [6] K. L. Kim *et al.*, "The design and testing of a cooling system using mixed solid cryogen for a portable superconducting magnetic energy storage system," *Supercond. Sci. Technol.*, vol. 23, no. 12, p. 125006, Dec. 2010, doi: 10.1088/0953-2048/23/12/125006.
- [7] J. Kapek, K. Berger, and J. L  v  que, "2D and 3D validation of a hybrid method based on A and H formulations for Pulsed Field Magnetization," Nancy (Virtual), France, Jun. 2021. Accessed: Feb. 07, 2022. [Online]. Available: <https://hal.univ-lorraine.fr/hal-03273940>
- [8] L. Bortot *et al.*, "A Coupled A–H Formulation for Magneto-Thermal Transients in High-Temperature Superconducting Magnets," *IEEE Transactions on Applied Superconductivity*, vol. 30, no. 5, pp. 1–11, Aug. 2020, doi: 10.1109/TASC.2020.2969476.
- [9] J. Dular, K. Berger, C. Geuzaine, and B. Vanderheyden, "What Formulation Should One Choose for Modeling a 3D HTS Magnet Motor Pole with a Ferromagnetic Material?," in *23rd International Conference on the Computation of Electromagnetic Fields, Compumag 2021*, Cancun, Mexico, Jan. 2022, p. PA-A1: 14 (ID 179). Accessed: Mar. 03, 2022. [Online]. Available: <https://hal.archives-ouvertes.fr/hal-03539715>
- [10] G. Hajiri, K. Berger, and J. L  v  que, "Design and Testing of a New Cooling System using Solid Nitrogen for Pulsed Field Magnetization and Characterization of HTS Bulks," *J. Phys.: Conf. Ser.*, vol. 2043, no. 1, p. 012002, Oct. 2021, doi: 10.1088/1742-6596/2043/1/012002.
- [11] J. Kapek, K. Berger, M. R. Koblishka, F. Trillaud, and J. L  v  que, "2-D Numerical Modeling of a Bulk HTS Magnetization Based on H Formulation Coupled With Electrical Circuit," *IEEE Transactions on Applied Superconductivity*, vol. 29, no. 5, pp. 1–5, Aug. 2019, doi: 10.1109/TASC.2019.2897331.